Acta Mechanica 155, 27–43 (2002)

ACTA MECHANICA

Unified theory for parallel and focused beam nonspecular reflection at liquid-solid interfaces

T. E. Matikas, Athens, Greece

(Received January 11, 2001; revised April 2, 2001)

Summary. This paper presents a theoretical model based on wave mechanics for the reflection of focused and parallel ultrasonic beams from a liquid-solid interface. The incident beam is defined by a Gaussian velocity distribution along a plane emitter, and the reflected beam is described through its pressure field by means of asymptotic analysis based on the short wave hypothesis. In the case of a focused reflected beam, nonspecular phenomena are observed for any angle of incidence. However, in the case of a parallel reflected beam, nonspecular reflection only occurs if the incidence of the beam is in the neighborhood of the Rayleigh angle. The objective of this paper is to discuss in detail the physical mechanisms of nonspecular reflection for both focused and unfocused beams and to provide an understanding of the complex phenomena related to nonspecular reflection of ultrasonic beams, which plays an important role in scanning acustic microscopy for materials nondestructive characterization.

1 Introduction

Experimental studies of the reflection of a parallel acoustic beam incident on a plane water-metal [1] interface have shown that, for an incidence at or near the Rayleigh angle, the reflected profile exhibits an unexpectedly large width, a silent or minimum intensity zone and a lateral shift of the maximum intensity. The general features of the phenomenon have been described [2] as the result of the superposition of two parts: the usual geometric reflected beam and the acoustic field generated by reradiation of a leaky Rayleigh wave. Numerical calculations [3] of the profiles of the reflected beam yield similar results. An extension of the theory has been proposed using asymptotic analysis [4].

The interest in using ultrasonic focused beams for nondestructive evaluation (NDE) applications, particularly in the case of the reflection acoustic microscope, which is based on the principle of interaction of specular reflected waves with surface waves, has led to many recent studies of the reflection of focused beams. The theoretical model [5] deals with the reflection of convergent beams from a liquid-solid interface at Reyleigh angle incidence using the hypothesis of a well-collimated beam. The location of the focal point of the reflected beam was thus estimated, and both the lateral and axial displacements were predicted using an approximation for the reflected acousitc field. The axial displacement, which was predicted in the model [5], was imaged using schlieren photography [6]. Both the axial and lateral displacements were quantified experimentally [7] using ultrasonic imaging of the reflected beam. The developed model [5] has a number of advantages such as simplicity and amenability to an analytical solution, but it is difficult to apply it in its present form to beams having a more pronounced convergence, or to beams having an incidence other than the Rayleigh angle. Further, in the model [5] there is no notion of caustic of the incident or the reflected beams;

the only information about the distorted reflected field is the displacement of the focal point. Moreover, there is no physical explanation for the observed nonspecular phenomena; the model [5] does not differentiate this phenomenon from the one observed in case of the reflection of a parallel beam, where the leak in the liquid of a Rayleigh wave is responsible for the distortion of the reflected beam.

In a preceding paper [8] the previous theories were extended to include: (i) The incident beam was defined by its normal velocity distrubution along a plane emitter placed in the fluid, and the notion of the caustic of the acoustic beam was introduced. (ii) It was observed that for an incidence near the Rayleigh angle, where the phase of the reflection coefficient varies abruptly, the asymptotic method of steepest descent [9]–[11] (which was used in the case of the reflection of a parallel beam [4]) was not applicable. (iii) An asymptotic evaluation of the reflected pressure field was obtained for all angles of incidence and in particular for the Rayleigh angle. The asymptotic analysis, based on the short-wave assumption, was performed by means of the stationary phase method [9], [10], which was applied to the spatial Fourier representations. This allows one to explore the reflected pressure field in a region which is not limited to the fluid-solid interface alone, and thus to obtain a spatial representation of the reflected focused beam. (iv) Distortion of the caustic of the reflected beam was observed in the neighborhood of the Rayleigh angle incidence, including lateral and axial displacements of the focal point of the beam. At the Rayleigh angle incidence, the lateral displacement is maximum. At this particular angle the axial displacement is negligible in comparison to the lengh of the focal spot, and therefore it is not detectable experimentally. Moreover, other noncular phenomena were predicted for an incidence near the Rayleigh angle. These nonspecular phenomena include spreading of the reflected beam, asymmetric variation of the acoustic pressure about the axis, and curvature of the acoustic axis.

The goal of this paper is to provide a physical explanation of nonspecular phenomena and to compare the mechanisms of nonspecular reflection between focused and parallel beams. It is shown that the nonspecular reflection of a focused beam is due to the generation of a Rayleigh surface wave and occurs at any angle of incidence. For an incidence near the Rayleigh angle, the whole acoustic axis and a part of the caustic are distorted, including axial and lateral displacements of the focal point; for another incidence, a different part of the reflected beam will be modified. In this case, the presence of the Rayleigh pole of the reflection coefficient (singularity in the complex plane related to a leaky Rayleigh wave), does not affect the reflected beam. In other words, the reradiation of a leaky Rayleigh wave in the liquid, which was the main cause of nonspecular reflection of a parallel beam, is very low.

2 Theory of nonspecular reflection of a Gaussian parallel beam

2.1 Modeling the reflected parallel beam

Consider a Gaussian parallel bounded acoustic beam of characteristic width "a", incident on a plane liquid-solid interface at an angle θ_1. The normal velocity distribution along the emitting plane (which is defined by $z_i = 0$) is given by:

$$v_n(x_i, 0) = V_0 e^{-(x_i/a)^2} e^{-i\omega t}, \tag{1}$$

where V_0 denotes the central magnitude of v_n.

In Fig. 1, the liquid-solid interface is defined by $z = 0$. The half-space $z < 0$ is filled with a liquid with mass density ϱ and sound velocity c ($k = \omega/c$ denotes the wave number in the

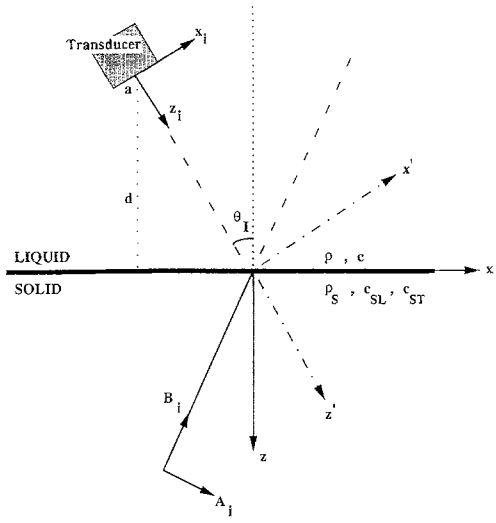

Fig. 1. Configuration of the problem and coordinate definition

liquid). The half-space $z > 0$ is an elastic solid with mass density ϱ_s and longitudinal and transversal wave velocities c_{SL} and c_{ST}, respectively.

The incident pressure field can be described as a plane-wave superposition of a Fourier integral with respect to the space variable $\bar{x}_i = x_i/a$:

$$P_{inc}(\bar{x}_i, \bar{z}_i) = \frac{\varrho c V_0 ka}{2\sqrt{\pi}} \int_{-\infty}^{+\infty} \frac{1}{\bar{k}_{z_i}} e^{(ka)^2 f_i(\bar{k}_{x_i})}\, d\bar{k}_{x_i} \tag{2}$$

with

$$f_i(\bar{k}_{x_i}) = -\frac{\bar{k}_{x_i}^2}{4} + \frac{i}{ka}\left(\bar{x}_i \bar{k}_{x_i} + \bar{z}_i \bar{k}_{z_i}\right), \tag{3}$$

where the bar denotes nondimensional parameters and $\bar{k}_{z_i}$ is a function of $\bar{k}_{x_i}$ through the dispersion relation.

The reflected pressure expressed in the system (x', z') is:

$$P_{ref}(\bar{x}', \bar{z}') = \frac{\varrho c V_0 ka}{2\sqrt{\pi}} \int_{-\infty}^{+\infty} \frac{R(\bar{k}_{x'})}{\bar{k}_{z'}} e^{(ka)^2 f_r(\bar{k}_{x'})}\, d\bar{k}_{x'} \tag{4}$$

with

$$f_r(\bar{k}_{x'}) = -\frac{\bar{k}_{x'}^2}{4} + \frac{i}{ka}\left(\bar{A}_i \bar{k}_{x'} + \bar{B}_i \bar{k}_{z'}\right), \tag{5}$$

where $\bar{A}_i$ and $\bar{B}_i$ are defined by the expressions:

$$\bar{A}_i = \bar{x}' \cos 2\theta_I + \bar{z}' \sin 2\theta_I\,, \qquad \bar{B}_i = \bar{x}' \sin 2\theta_I - \bar{z}' \sin 2\theta_I + \frac{d}{\cos\theta_I}\,. \tag{6}$$

$R(\bar{k}_{x'})$, in Eq. (4), denotes the plane-wave reflection coefficient [4], which is expressed in terms of the wave-number $\bar{k}_{x'}$ associated to the direction of the emitter. The reflection coefficient has a complex pole corresponding to the generalized Rayleigh wave, shown later in Eq. (21). At the Rayleigh angle, θ_R, this pole is purely imaginary:

$$\bar{k}_{p'} = i\frac{\bar{\alpha}_R}{\cos\theta_R}\,, \tag{7}$$

where $\bar{\alpha}_R$ is proportional to ϱ/ϱ_S.

2.2 *Application of the asymtotic method of steepest descent for an incidence at the Rayleigh angle*

Assuming a parallel beam with width large compared to the wave-length (short wave hypothesis: $ka >> 1$), the integral in Eq. (4) can then be evaluated asymptotically about the saddle-point, γ, of the function f_r [4]. The single complex saddle-point, which corresponds to the single direction of propagation of rays, is given by the expression:

$$\gamma = \frac{2i}{ka}\left(\bar{A}_i - \frac{\bar{B}_i\gamma}{\sqrt{1-\gamma^2}}\right). \tag{8}$$

Assuming that the pseudo-cooridinates $\bar{A}_1$ and $\bar{B}_i$ are of order 1, an analytical approximated expression for the saddle-point is obtained:

$$\gamma = i\frac{2\bar{A}_i}{ka} + \frac{4\bar{A}_i\bar{B}_i}{(ka)^2} + O\left(\frac{1}{(ka)^3}\right). \tag{9}$$

The saddle-point γ is located near the imaginary axis of the complex plane $\bar{k}_{x'}$.

The study of the topographic situation in the complex plane $\bar{k}_{x'}$, shown schematically in Fig. 2, enabled the asymptotic evaluation of the integral in Eq. (4) by means of the steepest-descent method [9], [10], and an analytical expression of the reflected pressure field at any point of the physical space was obtained [4]:

$$\begin{aligned} P_{ref}(\bar{x}', \bar{z}') = &- \varrho c V_0 e^{-\bar{A}_i{}^2} e^{i(ka)\bar{B}_i} \\ &+ \varrho c V_0 e^{-\bar{A}_i{}^2} e^{i(ka)\bar{B}_i}\left[2 - \frac{\sqrt{\pi}\,\bar{\alpha}_R(ka)}{\cos\theta_R}\exp\left(\frac{\bar{\alpha}_R(ka) - 2\bar{A}_i\cos\theta_R}{2\cos\theta_R}\right)^2\right] \\ &\bullet\ erfc\left(\frac{\bar{\alpha}_R(ka) - 2\bar{A}_i\cos\theta_R}{2\cos\theta_R}\right) + O\left(\frac{1}{ka}\right). \end{aligned} \tag{10}$$

According to Eq. (10), the reflected field depends only on two parameters, $\bar{\alpha}_R(ka)$ and $\bar{A}_i = (\bar{x} + \bar{z}\tan\theta_R)\cos\theta_R$, and is composed of two parts: (i) a first part that is purely geometrical, and (ii) a second part that contains non-geometrical terms corresponding to a leaky Rayleigh wave. The superposition of these two parts explains the nonspecular reflection of a parallel beam, which includes the spreading of the reflected beam, the presence of a null zone, and the displacement of the maximum of the reflected energy.

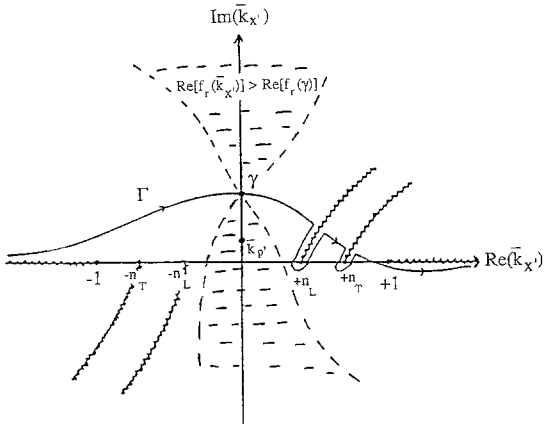

Fig. 2. Topographic situation in the complex $\bar{k}_{x'}$-plane in the case of a parallel beam. Location of the pole and the saddle-point for an incidence at the Rayleigh angle

3 Nonspecular reflection of a Gaussian focused beam

3.1 Modeling the reflected focused beam

Consider a focused ultrasonic beam, incident on a plane liquid-solid interface at an angle θ_I, (as shown in the configuration of Fig. 1). We assume a Gaussian profile of the normal velocity of particles along the emitting plane, $z_i = 0$,

$$v_n(x_i, 0) = V_o e^{-\left(\frac{x_i}{a}\right)^2} e^{-ik \sin\theta_0 \frac{x^2}{a}} e^{-i\omega t}, \tag{11}$$

where θ_o is the half angle of the convergent beam.

The incident pressure field is given by a Fourier integral [12]:

$$P_{inc}(\bar{x}_i, \bar{z}_i) = \frac{\varrho c V_0 \sqrt{ka}}{2\sqrt{i\pi \sin\theta_o}} \int_{-\infty}^{+\infty} \frac{e^{-\left[\frac{\bar{k}_{x_i}^2}{4\sin^2\theta_0}\right]}}{\bar{k}_{z_i}} e^{i(ka) f_i(\bar{k}_{x_i})} d\bar{k}_{x_i} \tag{12}$$

with

$$f_i(\bar{k}_{x_i}) = -\frac{\bar{k}_{x_i}^2}{4\sin\theta_0} + \bar{x}_i \bar{k}_{x_i} + \bar{z}_i \bar{k}_{z_i}. \tag{13}$$

The short wave hypothesis allows one to evaluate asymptotically the integral in Eq. (12) about the real saddle-points, γ_n, of the phase function f_i (which is defined as the roots of f_i'):

$$P_{inc}(\bar{x}_i, \bar{z}_i) = \text{const} \bullet \sum_n (\textit{term depending on } \gamma_n), \quad (n = 1) \quad \text{or} \quad (n = 1, 2, 3). \tag{14}$$

The reader can refer to [13] for detailed equations.

Equation (14) can be interpreted in terms of rays. The propagation around a point $(\bar{x}_{i0}, \bar{z}_{i0})$ can be locally assimilated to a plane wave of wave number:

$$\left[k\gamma_n, k\sqrt{1-\gamma_n^2}\right], \quad (n = 1) \quad \text{or} \quad (n = 1, 2, 3).$$

In these conditions, the direction of propagation is given by the straight line, which is defined by the equation:

$$D(\gamma_n) : (\bar{x}_i - \bar{x}_{i0})\gamma_n - (z_i - \bar{z}_{i0})\sqrt{1-\gamma_n^2} = 0.$$

The envelope of the set of all such lines defines the caustic of the field and represents the values of $\bar{x}_i$ and $\bar{z}_i$, for which two saddle-points are coincident. The mathematical expression

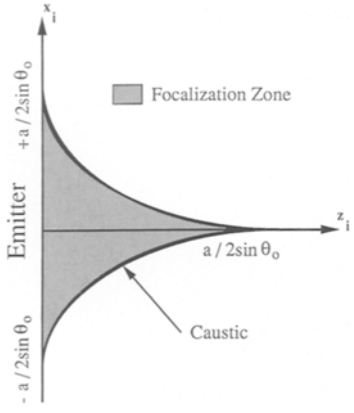

Fig. 3. The focal zone and the caustic of an incident beam

of the caustic can be obtained from the equations $f_i' = f_i'' = 0$. The caustic divides the physical space into two regions (shown schematically in Fig. 3):

(i) Region of a single stationary point, which is found outside the focal zone, where only a single ray passes through each physical point, and therefore, Eq. (14) has only one term. (ii) Region of three stationary points, which corresponds to the focal zone, where three rays pass through each point, two of these rays are tangent to the "near" branch of the caustic, and the third ray is tangent to the "further" branch of the caustic, therefore, Eq. (14) has three terms.

In order to evaluate the reflected field, it is convenient to write the continuity conditions in the (x, z) coordinate system, which it is done by multiplying the integrand of Eq. (12) by the plane-wave reflection coefficient for a liquid-solid interface, $R(\bar{k}_x)$, then to express the equations in the (x', z') coordinate system. Hence, the reflected pressure field is given by:

$$P_{ref}(\bar{x}, \bar{z}) = \frac{\varrho c V \sqrt{ka}}{2\sqrt{i\pi \sin\theta_o}} \int_{-\infty}^{+\infty} R(\bar{k}_x) \frac{e^{-\left[\frac{(\bar{k}_x \cos\theta_I - \bar{k}_z \sin\theta_I)^2}{4\sin^2\theta_0}\right]}}{\bar{k}_z} e^{i(ka)\tilde{f}_r(\bar{k}_x)} d\bar{k}_x \tag{15}$$

with

$$\tilde{f}_r(\bar{k}_x) = \frac{(\bar{k}_x \cos\theta_I - \bar{k}_z \sin\theta_I)^2}{4\sin\theta_0} + (x + \bar{d}\tan\theta_I)\,\bar{k}_x + (\bar{d} - \bar{z})\,\bar{k}_z\,. \tag{16}$$

With the assumption $\varrho/\varrho_s << 1$, which implies that the density of the liquid is much smaller than the density of the solid and is satisfied in most cases, the relection coefficient has a complex pole, $\bar{k}_p$, in the $\bar{k}_x$-plane that can be written in the form:

$$\bar{k}_p = \bar{k}_R + i\bar{\alpha}_R\,, \qquad \bar{\alpha}_R << 1\,, \tag{17}$$

where $\bar{k}_R = \sin\theta_R$ (θ_R is the Rayleigh angle) and $\bar{\alpha}_R$ is proportioal to ϱ/ϱ_s.

For an incidence near the Rayleigh angle, the reflection coefficient may be written in an approximated form, which is obtained by a Laurent series expansion about the Rayleigh singularity:

$$R(\bar{k}_x) = \frac{\bar{k}_x - \bar{k}_0}{\bar{k}_x - \bar{k}_p}\,. \tag{18}$$

In the case of absence of losses in the medium, the zero, $\bar{k}_0$, of the reflection coefficients is the complex conjugate, $\bar{k}_p^*$, of the pole. The function $\bar{k}_z = \sqrt{1 - \bar{k}_x^2}$ has two branch points at $\bar{k}_x = \pm 1$. Figure 4 shows the real integration path in the coordinate system (x, z); the dotted line represents the path in the second plane of Riemann. The physical meaning of that path can be understood by looking at Fig. 5. In Fig. 5, the line D, which corresponds to $(\bar{k}_x, \bar{k}_z) = (1, 0)$, separates the physical half-space $z_i > 0$ into two regions:

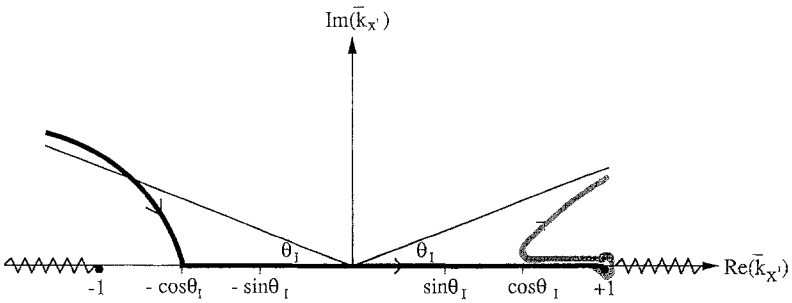

Fig. 4. Initial integration path for the acoustic pressure integral representation, in the system (x, z)

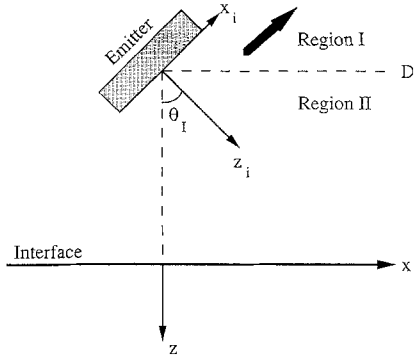

Fig. 5. Configuration of the problem showing the different wave propagation possibilities

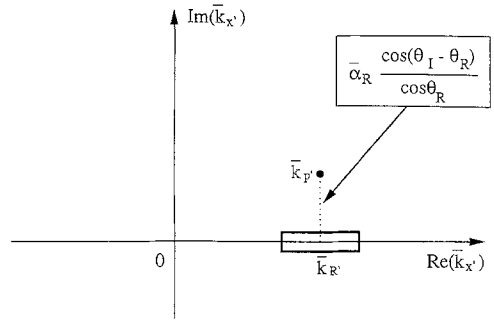

Fig. 6. Location of the pole of the reflection coefficient in the complex $(\bar{k}_{x'}, \bar{k}_{z'})$ plane, for an angle of incidence different from the Rayleigh angle ($\bar{k}_{R'} \neq 0$). The rectangle indicates the area of influence of the Rayleigh pole

Region (I): in which $\mathrm{Re}\,(\bar{k}_z) < 0$, with propagation along the z negative (part of the path shown as a dotted curve in Fig. 4, situated in the second plane of Riemann).

Region (II): in which $\mathrm{Re}\,(\bar{k}_z) > 0$, with propagation along the z positive (part of the path shown as a continuous curve in Fig. 4, situated in the first plane of Riemann).

Finally, the reflected pressure field expressed in the (x', z') coordinate system is given by:

$$P_{ref}(\bar{x}', \bar{z}') = \frac{\varrho c V_0 \sqrt{ka}}{2\sqrt{i\pi \sin\theta_0}} \int_{-\infty}^{+\infty} R(\bar{k}_{x'}) \frac{e^{-\left[\frac{\bar{k}_{x'}^2}{4\sin^2\theta_0}\right]}}{\bar{k}_{z'}} e^{i(ka) f_r(\bar{k}_{x'})}\, d\bar{k}_{x'} \tag{19}$$

with

$$f_r(\bar{k}_{x'}) = \frac{\bar{k}_{x'}^2}{4\sin\theta_0} + \bar{A}_i \bar{k}_{x'} + \bar{B}_i \bar{k}_{z'}\,, \tag{20}$$

where $\bar{A}_i$ and $\bar{B}_i$ are defined in Eq. (6).

In the coordinate system (x', z'), the Rayleigh pole is given by the expression:

$$\bar{k}_{p'} = \sin(\theta_I - \theta_R) + i \frac{\bar{\alpha}_R}{\cos\theta_R} \cos(\theta_I - \theta_R) \tag{21}$$

with $\bar{k}_{R'} = \sin(\theta_I - \theta_R)$ denoting the real part of this pole (Fig. 6.)

For the special case of the Rayleigh angle incidence ($\theta_I = \theta_R$), the pole becomes purely imaginary, as shown in Eq. (7). In the neighborhood of the pole, the reflection coefficient $R(\bar{k}_{x'})$ is given by an approximated expression:

$$R(\bar{k}_{x'}) = \frac{\bar{k}_{x'} - \bar{k}_{p'}^*}{\bar{k}_{x'} - \bar{k}_{p'}}\,. \tag{22}$$

where $\bar{k}_{p'}^*$ is the complex conjugate of the pole $\bar{k}_{p'}$.This approximation, with $\bar{\alpha}_R \ll 1$, is valid in a domain of the $\bar{k}_{x'}$-plane that includes a part of the real axis.

The reflection coefficinet can always be expressed in phase and modulus terms:

$$R(\bar{k}_{x'}) = \mu(\bar{k}_{x'})\, e^{i\varphi(\bar{k}_{x'})}\,. \tag{23}$$

Figure 7 shows the modulus, $\mu(\bar{k}_{x'})$, and the phase, $\varphi(\bar{k}_{x'})$, of the reflection coefficinet for a water-aluminum interface. Using the approximation given in Eq. (22) it can be concluded that the modulus of the reflection coefficient, in the neighborhood of the Rayleigh pole, tends toward infinity, whereas the phase is regular as long as $\mathrm{Re}\,(\bar{k}_{x'}) = 0$.

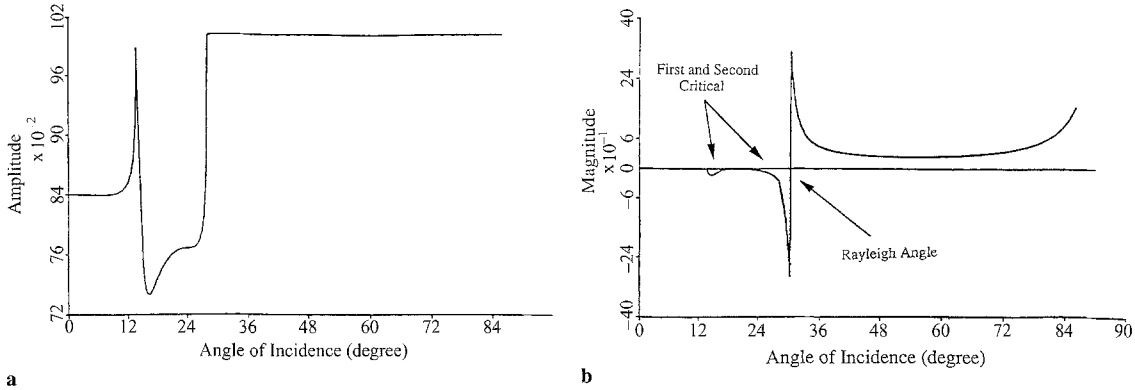

Fig. 7a. Modulus of the reflection coefficient for a liquid-solid plane interface; **b** Phase of the reflection coefficient for a liquid-solid plane interface

3.2 Asymptotic analysis

Assuming that the characteristic width of the acoustic beam "a" is large compared to the emission wavelength $\lambda = 2\pi/k(ka >> 1)$, the reflected pressure field, given by Eq. (19), may be evaluated by means of an asymptotic method. In order to evaluate asymptotically the integral in Eq. (19), the reflection coefficient will be represented in terms of modulus and phase, and the phase part will be regrouped with the function f_r. Next, it will be shown that the straightforward steepest descent method is not applicable in the case of a reflected focused beam because it is not uniformly valid in the neighorhood of the Rayleigh angle, and therefore, the asymptotic method of stationary phase will be used.

Assume that the integral in Eq. (19) can be evaluated analytically by applying the steepest descent method, hence, the asymptotic expansion for the reflected field, Eq. (19), at order 2 is given by [13]:

$$P_{ref}(\bar{x}', \bar{z}') = \frac{\varrho c V_0 \sqrt{ka}}{2\sqrt{i\pi}\sin\theta_o} e^{ikaf(\gamma_n)} \left\{ \left(\frac{-2\pi}{ikaf''(\gamma_n)} \right)^{1/2} q(\gamma_n) \right.$$

$$+ \frac{\sqrt{\pi}}{4(ka)^{3/2}} \left[\frac{i}{8} \left(\frac{2i}{f''(\gamma_n)} \right)^{5/2} \left(f^{(4)}(\gamma_n) - \frac{5}{3} \frac{(f'''(\gamma_n))^2}{f''(\gamma_n)} \right) q(\gamma_n) \right.$$

$$\left. \left. - \frac{2if'''(\gamma_n)}{(f''(\gamma_n))^2} \left(\frac{2i}{f''(\gamma_n)} \right)^{1/2} q'(\gamma_n) + \left(\frac{2i}{f''(\gamma_n)} \right)^{3/2} q''(\gamma_n) \right] \right\} + O\left(\frac{1}{(ka)^{5/2}} \right), \tag{24}$$

where

$$q(\gamma_n) = R(\gamma_n) \frac{\exp\left[-\dfrac{\gamma_n^2}{4\sin^2\theta_0} \right]}{\sqrt{1-\gamma_n^2}}.$$

The subscript "n" denotes summation for the real saddle-points ($n = 3$ for points inside the caustic of the reflected beam and $n = 1$ for points outside the caustic).

Equation (24) has two terms of the order $(ka)^{-1/2}$ and $(ka)^{-3/2}$ (terms of the order $(ka)^{-5/2}$ or smaller are omitted), which contain the bounded functions $q(\gamma_n)$, $R(\gamma_n)$, $f''(\gamma_n)$, $f'''(\gamma_n)$. The second term of the asymptotic expansion (24) contains the function $q'(\gamma_n)$, which, after expansion of the reflection coefficient in terms of phase and modulus, can be developed as:

$$q'(\gamma_n) = \left[\frac{\mu'(\gamma_n)}{\mu(\gamma_n)} + \varphi'(\gamma_n) \right] q(\gamma_n) + \text{terms of order } 1. \tag{25}$$

For an incidence in the neighborhood of the Rayleigh angle, as it is discussed before, the phase of the reflection coefficient varies repidly, hence, the derivative of the phase reaches high levels. This is the case where at least one saddle-point verifies the following condition:

$$\frac{|\varphi'(\gamma_n)|}{(ka)^{3/2}} \approx \frac{1}{(ka)^{1/2}} \,. \tag{26}$$

Therefore, the second term of the expansion (24) may become comparable to, or even greater than, the first one. In this case, the saddle-point method cannot be used because it is not uniformly valid near the Rayleigh angle.

The consition illustrated in Eq. (26) corresponds to:

$$\frac{|\varphi'(\bar{k}_{x'})|}{ka} \approx 1 \,, \tag{27}$$

where $\bar{k}_{x'}$ satisfies:

$$|\bar{k}_{x'} - \bar{k}_{R'}| << \varepsilon \tag{28}$$

with ε a small parameter that depends on ϱ_s/ϱ.

The function $\varphi'(\bar{k}_{x'})$ is bounded by $\varphi'(\bar{k}_{R'})$, which is of the order ϱ_s/ϱ, so the condition (28) implies that:

$$(ka)\left(\frac{\varrho}{\varrho_s}\right) << 1 \,. \tag{29}$$

In order to apply an asymptotic method and be able to describe the nonspecular phenomena, it is therefore necessary to express the reflection coefficient in terms of phase and modulus and to regroup the phase with the function f_r:

$$\hat{f}_r(\bar{k}_{x'}) = f_r(\bar{k}_{x'}) + \frac{\varphi(\bar{k}_{x'})}{ka} \,. \tag{30}$$

However, the function $\hat{f}_r$, being an argument function is not holomorphic. So, the steepest descent method cannot be applied in the case of the reflected field, since this asymptotic method is based on the Cauchy theorem and is only applicable to holomorphic functions. However, $\bar{k}_{x'}$ may be assumed to be real, so, considering the integration on the real axis where $\hat{f}_r$ is analytic, the integral in Eq. (19) may be evaluated by applying the asymptotic method of stationary phase.

The principle of stationary phase asserts, that, as $ka \to \infty$, the dominant terms in the asymptotic expansion of the integral in Eq. (19) (where $\hat{f}_r(\bar{k}_{x'})$ is real) arise from the immediate neighborhood of the points at which the phase $(ka)\hat{f}_r(\bar{k}_{x'})$ is stationary. Assuming that the coefficients $\bar{A}_i$ and $\bar{B}_i$ in the functions $\hat{f}_r$ are of order 1, the reflected pressure is given by [8]:

$$R_{ref}(\bar{x}_0', \bar{z}_0') = \sum_n \frac{\varrho c V_0 e^{-i\pi/2} \varrho(\hat{\gamma}_n)}{\sqrt{-2\sin\theta_o \hat{f}_r''(\hat{\gamma}_n)}} \frac{\exp\left[\dfrac{-\hat{\gamma}_n{}^2}{4\sin^2\theta_0} + \dfrac{i(ka)\,\hat{\gamma}_n{}^2}{4\sin\theta_0}\right]}{\sqrt{[1-\hat{\gamma}_n{}^2}}$$
$$\bullet \exp\left[i(ka)\left(\hat{\gamma}_n \bar{A}_i + \sqrt{1-\hat{\gamma}_n{}^2}\,\bar{B}_i\right)\right] + O\left(\frac{1}{ka}\right), \tag{31}$$

where $\hat{\gamma}_n$ are the real roots of the equation $\hat{f}_r{}' = 0$, and $(n = 1)$ or $(n = 1, 2, 3)$, depending on the location of the point $(\bar{x}_0{}', \bar{z}_0{}')$, whether it is situated outside or inside the focal zone of the reflected beam, respectively.

4 Mechanism of nonspecular phenomena

4.1 Case of a focused reflected beam

Figure 6 shows the location of the pole of the reflection coefficient, which is given by Eq. (21) in the $\bar{k}_{x'}$ complex plane for an incidence of the beam different than the Rayleigh angle ($\bar{k}_{R'}$ denotes the real part of the pole). For the Rayleight angle incidence, $\bar{k}_{R'} = 0$, the pole becomes purely imaginary as shown in Eq. (7). In Fig. 6, the rectangle around $\bar{k}_{R'}$ indicates the "influence area" of the Rayleigh pole, in other words the influence area of φ', such as defined in Eq. (28). The condition (26) is valid inside this area. Depending on the location of the points of interest in the reflected field (inside or outside the reflected focal zone which is limited by the caustic) two different cases may occur depending on the number of stationary points of the function $\hat{f}_r$. For points outside the focal zone, only one statioary point exists representing one ray, and corresponds to the single real root of the equation $\hat{f}_r' = 0$. For points inside the focal zone, three stationary points exist representing three different rays, and correspond to the existence of three real root of the equation $\hat{f}_r' = 0$. Figure 8 shows examples of the locations of physical points (shown in Fig. 8a) and the corresponding saddle-points (shown in Fig. 8b–8f). It must be noticed that when $\bar{A}_i$ changes its sign, the location of the corresponding saddle-points will be reversed with respect to the imaginary axis. For example, to the point D_2 located outside the focal zone for which $\bar{A}_i < 0$, correspond two complex saddle-points γ_1 amd γ_2 with positive real parts and one real saddle-point $\gamma_3 < 0$ (shown in Fig. 8f), whereas to the point D_3 located outside the focal zone for which $\bar{A}_i > 0$ correspond two complex saddle-points γ_1 and γ_2 with negative real parts and one real saddle-point $\gamma_3 > 0$ (shown in Fig. 8g).

The fundamental hypothesis here implies that, if at least one stationary point is situated inside the "influence area" of the Rayleigh pole (in other words, if at least one ray is incident at an angle near the Rayleigh angle), the generation of a Rayleigh surface wave will be accom-

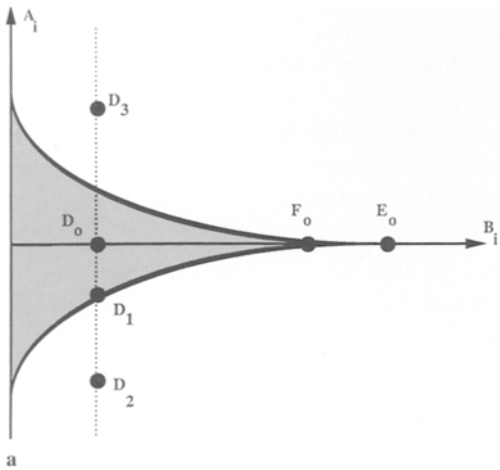

a

Fig. 8a. Location of various physical points in respect to the caustic of the focused beam:
Point F_0: focal point
Point D_0: located on the axic ($A_i = 0$) of the focused beam, inside the focal zone
Point D_1: located on the caustic of the focused beam, with $A_i < 0$
Point E_0: located on the axic ($A_i = 0$) of the focused beam and outside the focal zone
Point D_2: located outside the focal zone, with $A_i < 0$
Point D_3: located outside the focal zone, with $A_i > 0$
The position of the corresponding saddle-points (complex roots of f_r') is shown in Fig. 8b–8g

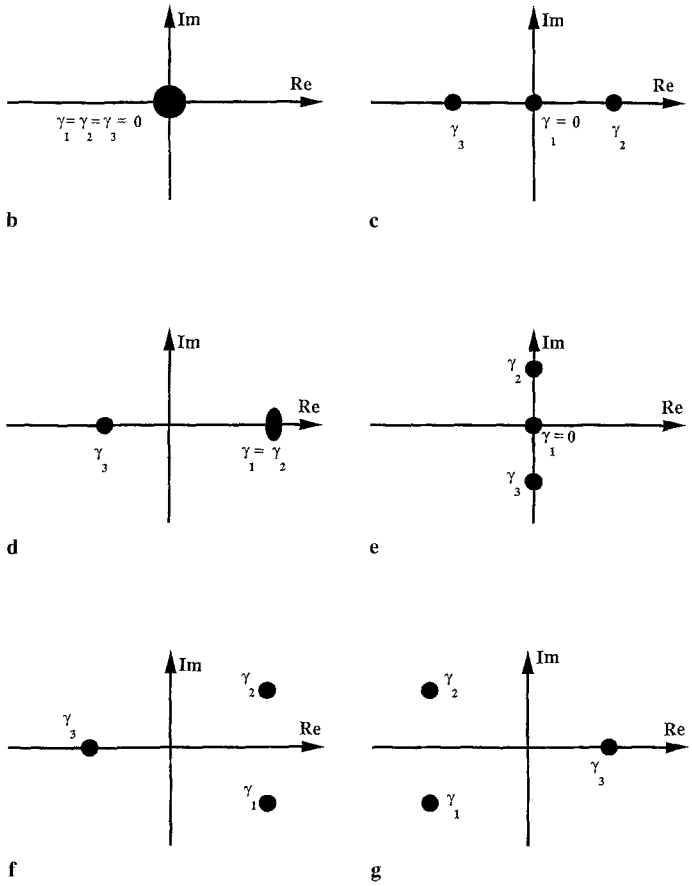

Fig. 8b. Three saddle-points: $\gamma_1 = \gamma_2 = \gamma_3 = 0$, which correspond to the focal point (point F_o); **c** Three saddle-points: $\gamma_1 = 0$; $\gamma_2 = -\gamma_3$, which correspond to the physical point D_0; **d** Three saddle-points: $\gamma_3 < 0$; $\gamma_1 = \gamma_2 > 0$, which correspond to the physical point D_1; **e** Two imaginary saddle-points, $\gamma_2 = -\gamma_3$, and one real, $\gamma_1 = 0$. which correspond to the physical point E_0; **f** Two complex saddle-points, γ_1, γ_2, with positive real parts and one real saddle-point, $\gamma_3 < 0$, which correspond to the physical point D_2; **g** Two complex saddle-points, γ_1, γ_2, with negative real parts and one real saddle-point, $\gamma_3 > 0$, which correspond to the physical point D_3

panied by a small displacement of the stationary point(s) of the specular beam, which translates to a small displacement of the geometrical reflected ray(s). This hypothesis leads to the assumption that the derivative of the second term in Eq. (30) has a very small value compared to the derivative of the first term. Using this assumption, a relation between specular and nonspecular stationary points can be finally obtained:

$$\hat{\gamma}_n = \gamma_n - \frac{\dfrac{\varphi'(\gamma_n)}{ka}}{f_r''(\gamma_n) + \dfrac{\varphi''(\gamma_n)}{ka}} = \gamma_n - \varepsilon' , \tag{32}$$

where ε' is a small parameter.

An immediate observation based on Eq. (32) is that, to any point of the "specular reflected beam" with coordinates $(\bar{A}_{i0}, \bar{B}_{i0})$, it can be associated an "image point" which belongs to the "nonspecular reflected field" with coordinates $(\hat{\bar{A}}_{i0}, \hat{\bar{B}}_{i0})$. It can also be observed that the points of the "specular reflected beam" are equivalent to the points of the "incident beam"

(according to Eqs. (13) and (20) the corresponding stationary points are the same). Using the same general procedure, a point on the nonspecular caustic of the reflected beam can be calculated from the corresponding point on the specular caustic.

The specular caustic is defined by $f_r' = f_r'' = 0$, where the function f_r is given by Eq. (20), and the points of the specular caustic $(\bar{A}_{i0}, \bar{B}_{i0})$ satisfy the equation:

$$\bar{A}_{i0}^{3/2} + \bar{B}_{i0}^{3/2} = \left(\frac{1}{2\sin\theta_0}\right)^{3/2}. \tag{33}$$

Similarly, the nonspecular caustic is defined by $\hat{f}_r' = \hat{f}_r'' = 0$, where the function f_r is given by Eq. (30), and the points $(\bar{\hat{A}}_{i0}, \bar{\hat{B}}_{i0})$ of the nonspecular reflected caustic satisfy the equation:

$$\left(\bar{\hat{A}}_{i0} + M\right)^{3/2} + \bar{\hat{B}}_{i0}^{3/2} = \left(\frac{1}{2\sin\theta_0} + N\right)^{3/2}, \tag{34}$$

where M and N are defined by the explicit expressions given in Eq. (36).

Using the equations $f_r' = 0$, $f_r'' = 0$, $\hat{f}_r' = 0$, $\hat{f}_r'' = 0$, and by expanding the derivative of the phase of the reflection coefficient $\varphi'(\bar{k}_x)$, which is contained in $\hat{f}_r$, about the saddle-points γ_i, the following expressions are obtained:

$$\begin{aligned} \bar{\hat{A}}_{i0} &= \bar{A}_{i0} - M - N{\gamma_n}^3, \\ \bar{\hat{B}}_{i0} &= \bar{B}_{i0} + N(1 - {\gamma_n}^2)^{3/2}, \end{aligned} \qquad (n = 1) \quad \text{or} \quad (n = 1, 2, 3) \tag{35}$$

where

$$M = \frac{1}{m}\sum_{i=1}^{m} \frac{\varphi'(\gamma_i) - \gamma_i\varphi''(\gamma_i)}{ka} \quad \text{and} \quad N = \frac{1}{m}\sum_{i=1}^{m} \frac{\varphi''(\gamma_i)}{ka}. \tag{36}$$

"m" denotes the number of stationary points in the neighborhood of $\bar{k}_R$.

Using Eq. (35) and for a given point on the specular caustic, the coordinates of the corresponding point of the nonspecular reflected caustic can be calculated.

Finaly, the position of the nonspecular point $(\hat{f}_r' = \hat{f}_r'' = \hat{f}_r''' = 0)$ can be calculated with respect to the specular focal point (which is obtained from the equations $f_r' = f_r'' = f_r''' = 0$):

$$\bar{\hat{A}}_{i0} = \bar{A}_{i0} - \frac{\varphi'(0)}{ka} \quad \text{and} \quad \bar{\hat{B}}_{i0} = \bar{B}_{i0} - \frac{\varphi''(0)}{ka} \tag{37}$$

$$\text{with} \quad \bar{A}_{i0} = 0 \quad \text{and} \quad \bar{B}_{i0} = \frac{1}{2\sin\theta_o}.$$

Hence, the lateral, L, and axial, A, displacements of the focal points can be quantified:

$$L = -\frac{\varphi'(0)}{ka} \quad \text{and} \quad A = \frac{\varphi''(0)}{ka}. \tag{38}$$

From the above analysis it can be concluded that it is always possible for a given "initial point" in the neighborhood of the specular reflected caustic situated in the interior (conversely at the exterior) of the specular focal zone, to determine a corresponding "image point" that belongs to the nonspecular reflected beam situated at the exterior (conversely in the interior) of the nonspecular focal zone. In this case, three stationary points (conversely a single stationary point) correspond to the initial point, and a single stationary point (conversely three stationary points) corresponds to the image point.

As an example, consider two points, M_1, and M_2, situated at the exterior and in the neighborhood of the specular reflected caustic (as shown in Fig. 9a), near which passes a single ray.

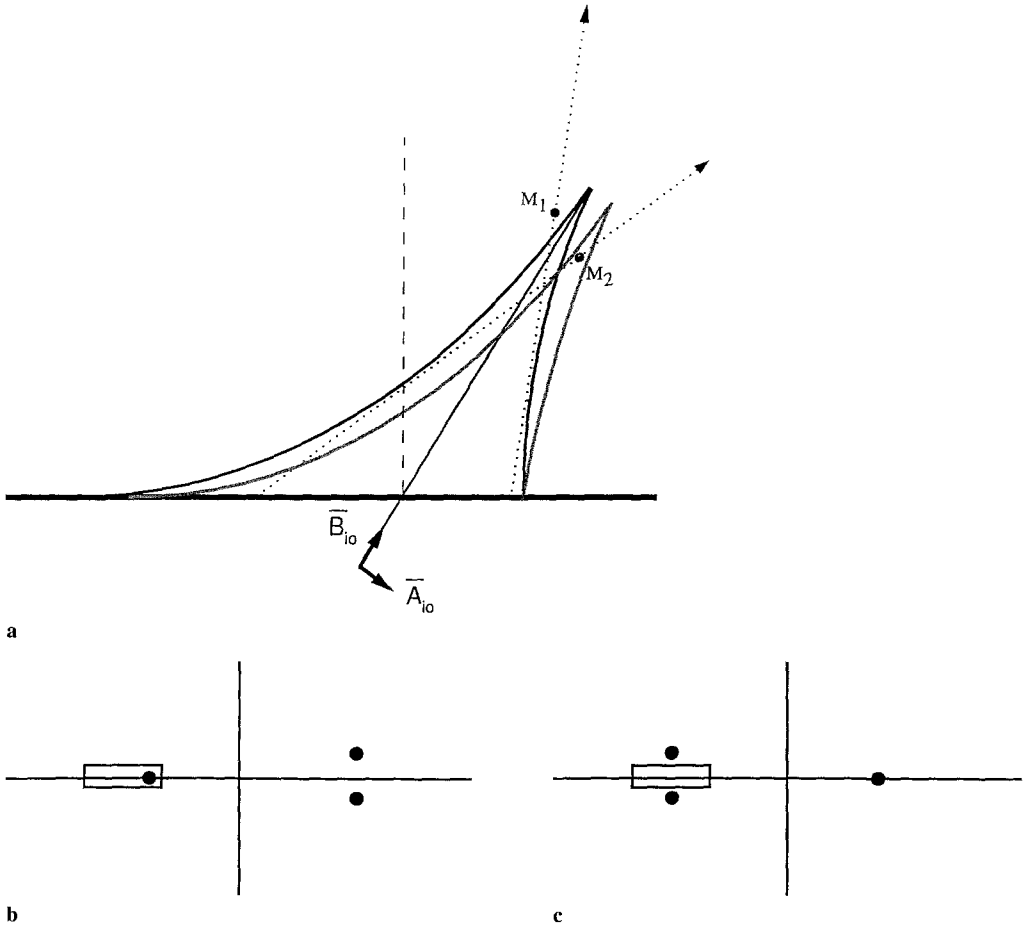

Fig. 9a. Points M_1 (with $A_i < 0$) and M_2 (with $A_i > 0$) outside the specular reflected beam. The point M_2 is located inside the nonspecular reflected beam; **b** Point M_1: Location of the three roots of f_r' in the complex plane. Case similar to Fig. 8f; **c** Point M_2: Location of the three roots of f_r' in the complex plane. Case similar to Fig. 8g

The incidence of the beam is assumed to be near the Rayleigh angle. In order to calculate the image points M_1 and M_2 it must be considered that the corresponding ray will be slightly modified according to Eq. (32).

(a) From the point M_1 passes a ray with an angle far from the Rayleigh angle. From the corresponding image point will still pass a single ray. The positions of the complex roots of f_r' are shown in Fig. 9b. In this case, the corresponding roots to the initial point are: one real root (i.e., a single stationary point) and two complex roots situated far from the area of influence of the Rayleigh pole (as shown in Fig. 8), which implies that these roots will not be displaced and hence they will not become real.

(b) From the point M_2 passes a ray with an angle near Rayleigh angle. Therefore, three rays will pass from the corresponding image point. The positions of the complex root of f_r', are shown in Fig. 9c. In this case, the corresponding roots to the initial point are: one real root and two complex roots situated near the area of influence of the Rayleigh pole (as shown in Fig. 8), which implies that after a slight displacement they may become real. It can be concluded that, in this case, the image point could be situated in the interior of the nonspecular reflected caustic even if the initial point was located outside the speular caustic. This will result

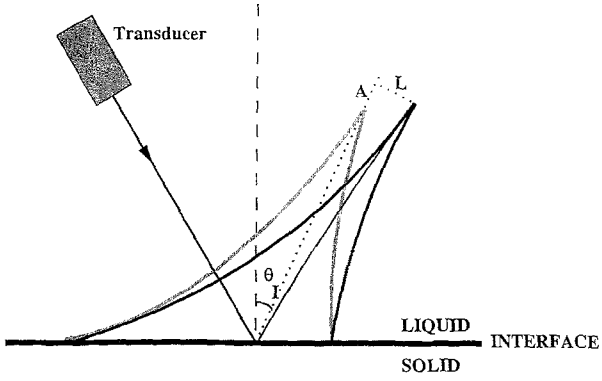

Fig. 10. Schematic representation of the distortion of the reflected caustic showing the lateral and axial displacements of the focal point, and the curvature of the acoustic axis of the reflected beam. The specular reflected caustic is shown in broken line and the nonspecular caustic in solid line

in a distortion of the caustic of the reflected beam. The caustic will be displaced to the right, and a curvature of the acoustic axis will occur (as shown in Fig. 10). In region I (where the point M_1 is situated) the gradient of the acoustic pressure will be lower than its values predicted by geometrical acoustics. In region II (where the point M_2 is situated) the gradient of the acousitc pressure will be greater than its value predicted by geometical acoustics. For this reason an asymmetric variation of the reflected pressure field around the axis is observed [8], [13]. These nonspecular phenomena have been verified experimentally in a previous work [7].

It is clearly shown from the analysis presented above that the nonspecular reflection of a focused beam is related to the phase part of the reflection coefficient. Nonspecular phenomena related to the reflection of focused beams are linked to the generation of a Rayleigh wave that is associated to a singularity near the real axis. The Rayleigh singularity zone on the real axis is displaced depending on the angle of incidence, therefore, for different angles of incidence the Rayleigh singularity zone will influence different parts of the reflected beam, in a way that there will always be distortion of a part of the reflected field. This local distortion of the reflected focused beam occurs for all the angles of incidence. In particular, for an incidence at the Rayleigh angle, where the real singularity is situated at zero, the distorted part of the reflected beam will include the region around the focal point together with a part of the caustic near the focal point.

The nonspecular phenomena that occur in the case of the reflection of a focused acoustic beam from a liquid-solid interface can be summarized as follows:

(a) For a beam incident near the Rayleigh angle, and if at least one ray passes from an observation point of the reflected beam at an angle (with the interface) near the Rayleigh angle, the corresponding acoustic pressure at this point will be modified with respect to its specular value. In other words, nonspecular reflection occurs for all physical points for wich at least one stationary point remains in the neighborhood of zero (note that the real part of the Rayleigh pole in the (x', z') coordinate system is equal to zero, for an incidence of the beam equal to the Rayleigh angle). Among the points of the physical space concerned here are (see Fig. 10):

- A region around and on the focal point (for which three stationary points are equal to zero); the corresponding nonspecular phenomena include lateral and axial displacements of the specular reflected focal point.
- A region around and on the part of the caustic situated near the focal point (were three stationary points are near zero); the coresponding nonspecular phenomena include distortion of the causic, spreading of the reflected beam, and asymmetric variation of the acoustic pressure around the reflected caustic.

- A region around and on the acoustic axis (for which on stationary point is always equal to zero); the corresponding nonspecular phenomena include curvature of the acoustic axis.

It should be noted that there always exist points of the reflected beam, to which a set of stationary points situated far from zero can be associated. The acoustic pressure at these points will be specular in spite of the fact that the beam is incident at an angle in the neighborhood of the Rayleigh angle.

(b) In the case of an incidence far from the Rayleigh angle, the real part of the Rayleigh pole will be far from zero. Therefore, points like the focal point (for which three stationary points are equal to zero) will now be reflected specularly. However, points of the reflected field always exist for which at least one stationary point remains in the neighborhood of the new real part of the Rayleigh pole (which is different from zero). The reflected field at these points will be nonspecular (modified with respect to values predicted by geometric acoustics), in spite of an incidence far from the Rayleigh angle. An example of this case is a part of the caustic situated far from the focal point that will be reflected nonspecularly.

4.2 Case of a parallel reflected beam

In the case of the reflection of a parallel beam, considering the coordinate system (x', z'), the single saddle-point moves on the imaginary axis, $\mathrm{Im}[\bar{k}_{x'}]$, hence it passes necessarily through the pole $\bar{k}_{p'}$ (as shown in Fig. 2). The Rayleigh pole is a singularity in the complex plane linked to the leakage of a Rayleigh surface wave in the liquid. In the case, nonspecular phenomena are related to the singulartiy of the modulus of the reflection coefficient (when $\bar{k}_{x'} = \bar{k}_{p'}$, then $|R| \to \infty$). This is justified by the presence of the complemantary error function, $erfc[\gamma - \bar{k}_{p'}]$, in the analytical expressions of the reflected pressure field (see Eq. (10)). This term does not exist in the expression of the reflected pressure of a focused beam.

Nonspecular phenomena related to the "phase phenomenon" also exist in the case of the reflection of a parallel beam, but they are negligible compared to nonspecular phenomena related to the "amplitude phenomenon". By expressing the reflection coefficient, $R(\bar{k}_{x'})$, in terms of modulus $\mu(\bar{k}_{x'})$ and phase $\varphi(\bar{k}_{x'})$, the Fourier integral in Eq. (4) which describes the pressure field of a reflected parallel beam in the (x', z') coordinate system can be written in the form:

$$P_{ref}(\bar{x}', \bar{z}') = C \int_{-\infty}^{+\infty} \mu(\bar{k}_{x'})\, F(\bar{k}_{x'}) \exp\left[i(ka)^2 \left(f_r(\bar{k}_{x'}) + H(\bar{k}_{x'})\right)\right] d\bar{k}_{x'}\,, \tag{39}$$

where $f_r(\bar{k}_{x'})$ is given by Eq. (5), and

$$H(\bar{k}_{x'}) = \frac{\varphi(\bar{k}_{x'})}{(ka)^2}\,. \tag{40}$$

It can be observed that in the case of the reflection of a parallel beam the term $H(\bar{k}_{x'})$, which could produce nonspecular phenomena related to the "phase phenomenon", is negligible; for $ka \gg 1 \Rightarrow H(\bar{k}_{x'}) \ll f_r(\bar{k}_{x'})$. Note that in the case of the reflection of a focused beam (where the "phase phenomenon" is predominant) the term related to nonspecular reflection is inversely proportional to (ka), as it is obvious from Eq. (30). Also, in the case of a focused beam, when the saddle-point(s) is (are) displaced, the derivative of the phase of the reflection coefficient, $\varphi(\bar{k}_{x'})$, varies a lot more rapidly than in the case of a parallel beam [13].

4.3 Remark on the influence of the liquid-solid interface on the nonspecular reflection of acoustic beams

The analysis presented in this paper that led to the quantification of nonspecular phenomena was based on the condition shown in Eq. (29). In the context of the short wave hypothesis, $ka \gg 1$, and by taking Eq. (29), into accound it is obvious that for a given value of (ka) nonspecular phenomena occur when the condition $\varrho \ll \varrho_s$ is satisfied. This leads to the conclusion that the higher the attenuation of the Rayleigh waves is, the less significant will be the nonspecular phenomena. However, for a given interface (ϱ/ϱ_s is fixed), the significance of nonspecular phenomena is inversely proportional to (ka), see Eqs. (29), (30) and (38). In other words, the higher the ultrasonic frequency (which corresponds to higher attenuation of Rayleigh waves in the solid) is, the less significant will be the nonspecular reflection of the beam.

5 Conclusions

This paper presents a study of the structure of the acousitc field when a Gaussian beam (parallel or focused) is reflected from a plane liquid-solid interface. The incident beam is modeled by a plane-wave decomposition using the Fourier integral representation. The reflected pressure field is described in a coordinate system corresponding to the emitter. In this convenient system, the expression of the phase function can be simplified in a way that the roots of its first derivative (called saddle-points) can be expressed in an analytical form. The reflected pressure itegral is then evaluated by means of asymptotic analysis using the steepest descent method in the case of a parallel reflected beam, or the stationary phase method in the case of a focused reflected beam. This asymptotic analysis is based on the short wave hypothesis, and an analytical, uniformly valid expression for any angle of incidence can be obtained finally.

In the case of a focused beam, a modification of the structure of the reflected field with respect to values predicted by geometric acoustics was observed for any angle of incidence. In particular, for an incidence in the neighborhood or equal to the Rayleigh angle, nonspecular phenomena involve a part of the caustic of the reflected beam including the focal point, and the entire acoustic axis. Simple expressions of the axial and lateral displacements of the focal point were obtained leading to numerical quantification of the phenomena. These analytical results are in agreement with experimental data reported in the literature [7].

The study of the reflection of a parallel beam enables one to compare the nonspecular reflection of focused and unfocused beams. It was found that in the case of a parallel beam the mechanism of nonspecular reflection is different from the case of a focused beam as it is summarized below:

(i) When a parallel ultrasonic beam is reflected from a liquid-solid interface (and in the context of geometric acousitcs), all energy (except the small quantity of diffracted energy) falls at the interface at the Rayleigh angle. Hence, generation of a Rayleigh surface wave occurs, and part of its energy is leaking back in the liquid producing the "amplitude phenomenon". In this case, the leakly Rayleigh wave is the principal mechanism of the wellknown related nonspecular phenomena.

(ii) However, in the case of a focused beam, only a part of the energy falls onto the interface at the Rayleigh angle. The abrupt variation of the phase of the reflection coefficient in the neighborhood of the Rayleigh angle causes a local modification of the reflected beam. Here, the "phase phenomenon" is more important than the reradiation of a leaky Rayleigh

wave in the liquid. The same "phase phenomenon" is also present in the case of the reflection of a parallel beam, but it is much less significant than the "amplitude phenomenon". Further, for a focused beam, a number of rays always fall onto the interface at the Rayleigh angle even if the beam incidence is far from the Rayleigh angle. For this reason, there will always be areas of the reflected focused beam that are distorted.

References

[1] Breazeale, M. A., Adler, L., Scott, G. W.: Interaction of ultrasonic waves incident at the Rayleigh angle onto a liquid-solid interface. J. A. P. **48,** 530–537 (1977).
[2] Bertoni, H. L., Tamir, T.: Unified theory of Rayleigh-angle phenomena for acoustic beams at liquid-solid interfaces. Appl. Phys. **2,** 157–172 (1973).
[3] Ngoc, T. D. K., Mayer, W. G.: Numerical integration method for reflected beam profiles near Rayleigh angle. J. Acoust. Soc. Am. **67,** 1149–1152 (1980).
[4] Rousseau, M., Gatignol, P.: Short wave analysis for the reflection of bounded acoustic beams onto liquid-solid interfaces at the Rayleigh incidence. J. Acoust. Soc. Am. **78,** 1859–1867 (1985).
[5] Bertoni, H. L., Hsue, C. W., Tamir, T.: Nonspecular reflection of convergent beams form liquid-solid interface. Trait. Sign. **2,** 201–205 (1985).
[6] Nagy, P. B., Cho, C., Adler, L., Chimeriti, D.: Focal shift of convergent ultrasonic beams reflected from a liquid-solid interface. J. Acoust. Soc. Am. **81,** 835–839 (1987).
[7] Matikas, T. E., Rousseau, M., Gatignol, P.: Experimental study of focused ultrasonic beams reflected at a fluid-solid interface in the neighborhood of the Rayleigh angle. IEEE Trans. on Ultrasonics, Ferroelectrics and Frequency Control **39,** 737–744 (1992).
[8] Matikas, T. E., Rousseau, M., Gatignol, P.: Theoretical analysis for the reflection of a focused ultrasonic beam from a fluid-solid interface. J. Acoust. Soc. Am. **93,** 1407–1416 (1993).
[9] Roseau, M.: Asymptotic wave theory. North-Holland Series in Applied Mathematics and Mechanics, Vol. 20. Amsterdam: North-Holland 1976.
[10] Copson, E. T.: Asymptotic expansions. Cambridge : Cambridge University Press 1967.
[11] Ludwig, D.: Uniform asymptotic expansions at a caustic. Comm. Pure Appl. Math. **XIX,** 215–250 (1966).
[12] Rousseau, M., Gatignol, P.: Etude asymptotique d'un faisceau Gaussien focalise. J. Acoustique **1,** 95–99 (1988).
[13] Matikas, T. E.: Theoretical and experimental study of the interaction of focused ultrasonic beams with plane fluid-solid interfaces. Application at the analysis of the state of material surfaces. Universite de Technologie de Compiegne, France 1991.

Author's address: T. E. Matikas, Greek Atomic Energy Commission, P.O.Box 60092, 153 10 Agia Paraskevi Attikis, Athens, Greece